PERGAMON

International Journal of Heat and Mass Transfer 45 (2002) 2449–2463

International Journal of HEAT and MASS TRANSFER

www.elsevier.com/locate/ijhmt

Forced convective boiling of pure refrigerants in a bundle of enhanced tubes having pores and connecting gaps

Nae-Hyun Kim *, Jin-Pyo Cho, Baek Youn

Department of Mechanical Engineering, University of Inchon #177 Dohwa-Dong, Nam-Gu, Inchon, 402-749, Republic of Korea

Received 26 April 2001; received in revised form 7 November 2001

Abstract

In this study, convective boiling tests were conducted for enhanced tube bundles. The surface geometry consists of pores and connecting gaps. Tubes with three different pore sizes ($d_p = 0.20$, 0.23 and 0.27 mm) were tested using R-123 and R-134a for the following range: 8 kg/m^2 s $\leqslant G \leqslant$ 26 kg/m^2 s, 10 kW/m^2 $\leqslant q \leqslant$ 40 kW/m^2 and $0.1 \leqslant x \leqslant 0.9$. The convective boiling heat transfer coefficients were strongly dependent on heat flux with negligible dependency on mass flux or quality. For the present enhanced geometry (pores and gaps), the convective effect was apparent. The gaps of the present tubes may have served routes for the passage of two-phase mixtures, and enhanced the boiling heat transfer. The convective effect was more pronounced at a higher saturation temperature. More bubbles will be generated at a higher saturation temperature, which will lead to enhanced convective contribution. The pore size where the maximum heat transfer coefficient was obtained was larger for R-134a ($d_p = 0.27$ mm) compared with that for R-123 ($d_p = 0.23$ mm). This trend was consistent with the previous pool boiling results. For the enhanced tube bundles, the convective effect was more pronounced for R-134a than for R-123. This trend was reversed for the smooth tube bundle. Possible reasoning is provided based on the bubble behavior on the tube wall. Both the modified Chen and the asymptotic model predicted the present data reasonably well. The RMSEs were 14.3% for the modified Chen model and 12.7% for the asymptotic model.

Keywords: Structured enhanced tube; Pore; Gap; Forced convective boiling; Bundle; R-123; R-134a

1. Introduction

In recent years, significant progress has been made in understanding the boiling heat transfer on the shell side of tube bundles. For a smooth tube bundle, it is well documented that the average boiling heat transfer coefficient of a bundle is significantly higher than that of a single tube, especially at low heat fluxes [1–3]. The convective two-phase flow in a bundle may account for this increase. At high heat fluxes, however, nucleate boiling effect dominates over convective effect, and the bundle heat transfer coefficient approaches that of a single tube. Similar results have been obtained for finned tube bundles [4,5].

For enhanced tube bundles, the trend is not so obvious. Available enhanced tube bundle data are listed in Table 1. In Table 1, bundle boiling heat transfer coefficients (h_b) are compared with pool boiling heat transfer coefficients (h_{nb}) at two different heat fluxes – one low (10–20 kW/m^2) and the other high (40–50 kW/m^2). The commercial tube name (if available) is written in the first column, followed by the tube classification as proposed by Kim and Choi [9]. Fig. 1 shows the classified tube geometry. Table 1 reveals that the bundle effect (defined as a bundle factor h_b/h_{nb}) is apparent for gapped tubes such as GEWA-SE and GEWA-K. No bundle effect is observed for porous coated tubes. For pored tubes such as Turbo-B, the bundle effect is not obvious. Memory et al. [7] obtained a strong bundle effect where as Gupte and Webb [6] obtained no bundle effect. From these

* Corresponding author. Tel.: +82-32-770-8420; fax: +82-32-770-8410.

E-mail address: knh0001@lion.inchon.ac.kr (N.-H. Kim).

0017-9310/02/$ - see front matter
PII: S0017-9310(01)00346-5

Nomenclature

A_{min}	minimum flow area in a bundle (m^2)
b	Reynolds number exponent in the friction correlation (dimensionless)
c_{pr}	specific heat of the refrigerant (J/kg K)
d	tube diameter (m)
d_b	bubble departure diameter (m)
d_p	pore diameter (m)
F	two-phase convective multiplier (dimensionless)
g	gravity (m/s^2) or gap width (m)
G	mass flux based on A_{min} (kg/m^2 s)
h	heat transfer coefficient (W/m^2 K)
h_b	convective boiling heat transfer coefficient in a bundle (W/m^2 K)
h_l	liquid-phase convective heat transfer coefficient (W/m^2 K)
h_{nb}	nucleate pool boiling heat transfer coefficient (W/m^2 K)
h_{nbb}	nucleate pool boiling heat transfer coefficient for one tube heated in a bundle (W/m^2 K)
h_{nbs}	convective boiling heat transfer coefficient on a single tube (W/m^2 K)
h_{fg}	latent heat of vaporization (J/kg)
H_t	tunnel height (m)
j_g	superficial gas velocity (m/s)
j_l	superficial liquid velocity (m/s)
k_l	thermal conductivity of liquid (W/m K)
m	Reynolds number exponent for the Nusselt number correlation (dimensionless)
$\dot{m}_r$	mass flow rate of the refrigerant (kg/s)
n	order of the asymptotic model (dimensionless)
N	number of data or number of active heaters upstream of the instrumented tube (dimensionless)
Nu_l	Nusselt number, dimensionless ($= h_l d/k_l$)
P_f	fin pitch (m)
P_{p1}	circumferential pore pitch (m)
P_{p2}	neighboring pore pitch (m)
Pr_l	liquid Prandtl number (dimensionless)
Pr_w	liquid Prandtl number at the wall temperature (dimensionless)
q''	heat flux (W/m^2)
Q_p	heat supplied to the pre-heater (W)
Q_H	heat supplied to a single in the test section (W)
Re_l	Reynolds number, dimensionless ($= dG(1-x)/\mu$)
$T_{p,in}$	refrigerant temperature at the pre-heater inlet (K)
$T_{p,sat}$	saturation temperature at the pre-heater (K)
T_{sat}	saturation temperature (K)
T_w	tube wall temperature (K)
W_t	tunnel width (m)
x	vapor quality (dimensionless)

Greek symbols

ρ_l	liquid density (kg/m^3)
ρ_g	vapor density (kg/m^3)
μ_l	dynamic viscosity of liquid (kg/ms)
μ_g	dynamic viscosity of vapor (kg/ms)
σ	surface tension (N/m)

results, one may suspect that the gaps may play an important role on the bundle effect, at a low heat flux at least. Two-phase mixtures which pass through the gaps may enhance the boiling heat transfer.

Kim and Choi [9] reported the pool boiling data for tubes having pores with connecting gaps. The enlarged photos of the surface geometry are shown in Fig. 1. The tubes yielded pool boiling heat transfer coefficients, which are approximately the same as those of pored tubes. In addition, their tubes did not show a dry-out in the sub-tunnel even at a high heat flux, which pored tubes usually do. They attributed the delay of the dry-out to the connecting gaps, which may have served additional routes for liquid supply. In a bundle, the gaps

Table 1
Previous studies on the bundle effect of enhanced tube bundles

Tubes	Tube classification	Refrigerant	T_{sat}(°C)	Bundle factor (h_b/h_{nb})		References
				Low q'' (10–20 kW/m^2)	High q'' (30–50 kW/m^2)	
GEWA-SE	Gaps	R-134a	4.4	>1.0	1.0	Gupte and Webb [6]
			26.7	>1.0	1.0	Gupte and Webb [6]
GEWA-K	Gaps	R-114	2.2	>1.0	>1.0	Memory et al. [7]
		R-114	2.2	>1.0	>1.0	Memory et al. [7]
Turbo-B	Pores	R-11	4.4	1.0	1.0	Gupte and Webb [6]
		R-123	26.7	1.0	1.0	Gupte and Webb [6]
Porous		R-114	2.2	1.0	1.0	Memory et al. [7]
Coated		R-113	47.6	1.0	1.0	Fujita et al. [8]

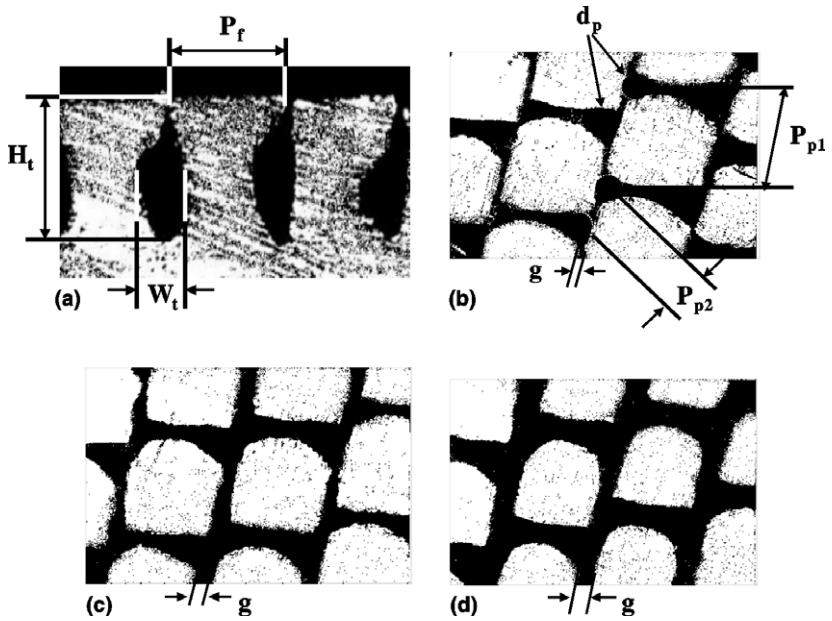

Fig. 1. Enlarged photos showing the present enhanced geometry: (a) cross-sectional view of the tunnel; (b) tube with $d_p = 0.20$ mm; (c) tube with $d_p = 0.23$ mm; (d) tube with $d_p = 0.27$ mm.

may also serve routes for the passage of two-phase mixtures, and enhance the boiling heat transfer. In their pool boiling study, Kim and Choi noticed that the optimum pore size differed for different refrigerants. We expect a similar trend in a bundle. Up to now, however, no investigation has been conducted on the effect of pore size on the forced convective boiling. In this study, the boiling characteristics in a bundle of enhanced tubes were investigated focusing on the effect of pore diameter. Obtained data are compared with existing convective boiling models.

2. Sample tubes

The same tubes as those used for the previous pool boiling test were used in this study. The surface geometry is shown in Fig. 1. These tubes were made from low integral fin tubes having 1654 fins/m with 1.3 mm fin height, cutting small notches (0.9 mm depth) on the fins, and then flattening the fins by a rolling process. The resultant tube had triangular pores with connecting gaps and gourd-shaped tunnels. Three tubes with different pore size (and corresponding gap width) were made. The pore size was varied by changing the pressure on the rollers. The geometric dimensions of the surfaces are listed in Table 2. The pore size in the table is represented by the diameter of a circle inscribed in a triangle. The geometric dimensions were measured from enlarged photos taken at 20 different locations. The pore size and the gap width were fairly uniform (±0.02 mm), and those listed in Table 2 are the averaged values.

3. Experimental apparatus

A schematic drawing of the apparatus is shown in Fig. 2, and the detailed drawing of the test section is shown in Fig. 3. The apparatus and the test section were made similar to those used by Gupte and Webb [6]. Refrigerant enters at the bottom of the test section at a known vapor quality. Heat is supplied to the tubes in the tube bundle by cartridge heaters. The two-phase mixture leaves the test section and goes to the condensers. Three condensers having 7.5 kW cooling capacity each are connected in parallel. The sub-cooled liquid then passes through a

Table 2
Geometric dimenions of the sample tubes

No.	d_p (mm)	g (mm)	P_{p1}	P_{p2}	P_f (mm)	H_t (mm)	W_t (mm)
1	0.20	0.04	0.71	0.374	0.605	0.54	0.25
2	0.23	0.07	0.71	0.384	0.605	0.54	0.25
3	0.27	0.10	0.71	0.400	0.605	0.54	0.25

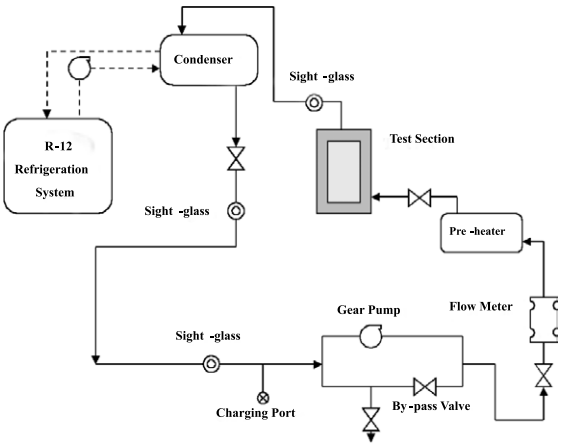

Fig. 2. Schematic drawing of the experimental apparatus.

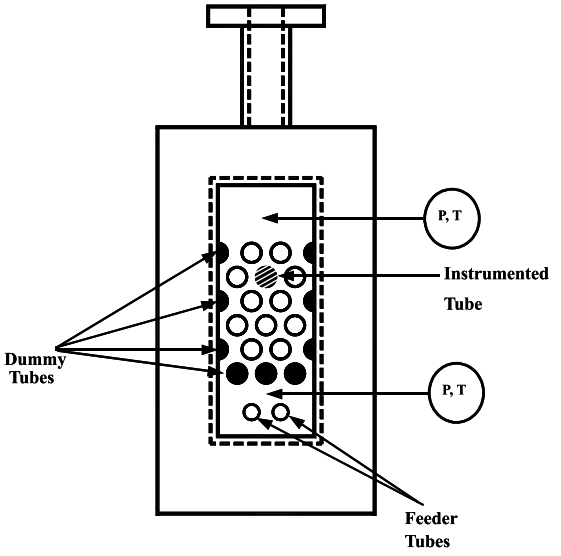

Fig. 3. Detailed drawing of the test section.

dryer, and goes to the magnetic pump having 1 gpm capacity. The mass flow meter (Micromotion DN25S-SS-1) is placed between the magnetic pump and the pre-heater to measure the mass flow rate. Heat is supplied to the pre-heater to obtain a known vapor quality. The two-phase mixture enters the test section through the feeder tubes located at the bottom of the tube bundle.

Heat input to the pre-heater determines the inlet vapor quality, which can be controlled independently. Since, the liquid loop is complete by itself, the mass flow rate can be controlled independently. Finally, the heat flux to the test tubes can be varied by regulating the line voltage to tubes. Thus, the apparatus was designed to control the vapor quality, mass velocity and heat flux independently.

Figs. 3 and 4 show the details of the test section and the instrumented tube, respectively. The enhanced tubes were specially made from thick-walled copper tubes of 18.8 mm outer diameter and 13.5 mm inner diameter. The length was 170 mm. Cartridge heaters of 13.45 mm diameter and 180 mm long were inserted into the test tubes. The heaters were specially manufactured to contain 170 mm long heated section (same length as that of the test tubes) and two 5 mm long unheated end sections. To minimize the heat loss, the unheated sections were covered with Teflon caps and Teflon rings as illustrated in Fig. 4. Before insertion, the heaters were coated with thermal epoxy to enhance the thermal contact with the tubes. The heaters were screwed into the back flange of the test section to form a staggered array of an equilateral triangular pitch of 23.8 mm. For that purpose, the heaters were specially manufactured to contain a male screw at one end. Heat was supplied to all the tubes except for those at the bottom row – its role was to develop flow in the tube bundle.

The instrumented tube was located at the center of the fifth row from the bottom. Fig. 4 shows the cross-section of the instrumented tube. The same tubes as those used by Kim and Choi [9] for the pool boiling test were used in the present study. The tubes have four thermocouple holes of 1.0 mm drilled to the center of the tube. Copper-constantan thermocouples of 0.3 mm diameter per wire were inserted into the holes to measure the tube wall temperature. Before insertion, the thermocouples were coated with a thermal epoxy (Chromalox HTRC) to provide good thermal contact with the tube wall. The thermal conductivity of the epoxy is close to that of aluminum. The steady state heat conduction equation was used to correct for the conduction temperature drop between the thermocouple and the boiling surface.

Saturation temperatures were measured at the top and the bottom of the tube bundle. Calibrated pressure transducers were also used to measure the saturation pressure at the same location. During the experiment, the saturation temperature calculated from the measured pressure was compared with the measured temperature, and they agreed within 0.2 °C. The measured

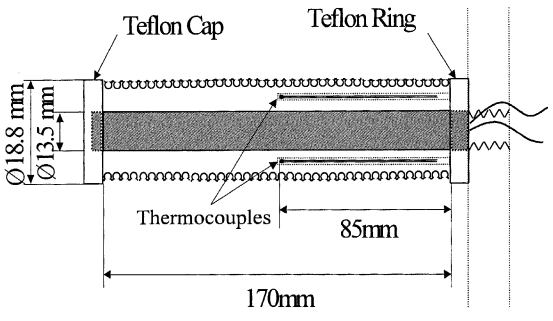

Fig. 4. Detailed sketch of the instrumented tube.

temperatures were used for data reduction. For convective boiling, the saturation temperature decreases along the flow passage due to the pressure loss. For the present experiment, the decrease was on the order of 0.5 °C. The saturation temperature at the instrumented tube was determined by linear interpolation of the top and bottom temperatures.

4. Experimental procedures

Before beginning the experiment, the apparatus was checked for possible leakage. The apparatus was kept under vacuum for 24 h, and the pressure rise was less than 10 kPa. While charging the system, a small amount of refrigerant was first introduced into the system. The system was then evacuated by a vacuum pump. This procedure was repeated several times before charging the system. Liquid refrigerant was introduced into the system from an inverted refrigerant drum to prevent any trapped gas in the drum entering the system. The absence of non-condensable gases was further confirmed by noting the agreement between the saturation temperature and the measured pressure in the test section.

Convective and pool boiling data were taken using R-123 and R-134a. For R-134a, data were taken at two saturation temperatures, 4.4 and 26.7 °C. For R-123, we could not steadily maintain 4.4 °C due to the limitations of the test facility, and only 26.7 °C data were taken. The mass flux was varied from 8 to 26 kg/m^2 s, heat flux from 10 to 40 kW/m^2 and vapor quality from 0.1 to 0.9. Data were taken first varying the vapor quality, and then heat flux, and then mass flux, all in a decreasing manner. The vapor quality at the instrumented tube location was determined from Eq. (1):

$$x = \left[\frac{Q_p + NQ_H}{\dot{m}_r} - c_{pr}(T_{p,sat} - T_{p,in})\right]. \quad (1)$$

Here, Q_p is the heat supplied to the pre-heater, Q_H is the heat supplied to a single heater in the test section, and N is the number of active heaters upstream of the instrumented tube. The test section and the pre-heater were heavily insulated to minimize the heat loss to the environment.

The heat transfer coefficient (h) was determined by the heat flux (q'') over wall superheat ($T_w - T_{sat}$). Calculations of q'' and h were based on the envelope area, defined by the heated length (170 mm) multiplied by the tube outside perimeter. The input power to the heater was measured by a precision watt-meter (Chitai 2402A) and the thermocouples were connected to the data logger (Fluke 2645A). The pressure transducers were also connected to the data logger. The thermocouples and the transducers were calibrated and checked for repeatability. The calculated accuracy of the temperature measurement was ±0.1 °C, heat flux measurement ±0.5%, mass velocity measurement ±1% and vapor quality measurement ±2%. An error analysis was conducted following the procedure proposed by Kline and McClintock [10]. The uncertainty in the heat transfer coefficient was estimated to be ±2% at the maximum heat flux (40 kW/m^2) and ±8% at a low heat flux (10 kW/m^2).

5. Results and discussion

5.1. Pool boiling in the bundle

Before running a convective boiling test, pool boiling tests were conducted for one heated tube in a bundle. To maintain the pool at a saturation condition, small amount of heat (0.2 kW) was supplied to the pre-heater. Increasing the pre-heater power to 0.5 kW did not affect the pool boiling results for the present bundle geometry. The present data (h_{nbb}) are compared with the single tube pool boiling data (h_{nbs}) by Kim and Choi [9], and the results are shown in Fig. 5. In the legend, the first notation denotes the pore size, the second one denotes the refrigerant, and the last one denotes the saturation temperature. The agreement is within ±20% for most of the data. Only one set of data ($d_p = 0.20$ mm, R-134a, $T_{sat} = 4.4$ °C) show approximately 25% difference. Gupte and Webb [6] compared their bundle pool boiling data with the single tube pool boiling data by Webb and Pais [11], and reported ±25% agreement for most of the data. For certain cases (GEWA-SE for R-123 and Turbo-B for R-11), however, they noticed 20–50% discrepancy.

5.2. Convective boiling in the smooth tube bundle

Prior to the tests on enhanced tube bundles, tests were conducted on a smooth tube bundle. To obtain

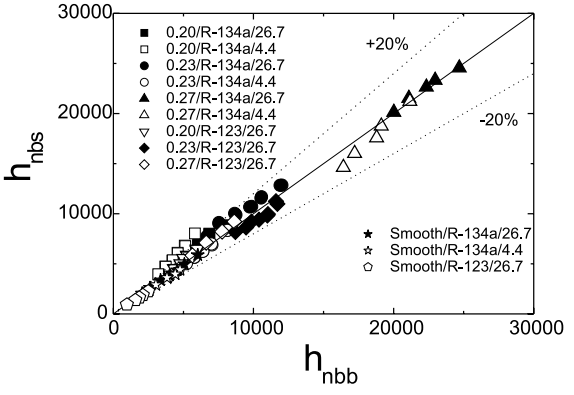

Fig. 5. The present pool boiling data (one heated tube in a bundle) compared with those by Kim and Choi [9] (single tube in a pool).

consistent results, the same smooth tube as that used by Kim and Choi [9] for the pool boiling test was used as the instrumented tube. In Fig. 6, boiling heat transfer coefficients are plotted against vapor quality for three different mass fluxes. Refrigerant used was R-134a and the saturation temperature was 4.4 °C. Each figure contains dotted lines, which represent the pool boiling heat transfer coefficients at the same heat flux. The pool boiling data shown in the figures are those obtained from the present apparatus. The maximum vapor quality that could be achieved in each experiment was limited by the experimental facility. For example, when the mass velocity was high, the maximum vapor quality obtained was approximately 0.5. If the heat input to the pre-heater had been increased, the saturation temperature would have increased, due to the limitations on the condenser of the present facility.

Fig. 6 shows that the heat transfer coefficient increases as the heat flux increases, and is almost independent on the vapor quality. Only at the high mass flux ($G = 26$ kg/m^2 s) combined with low heat flux ($q'' = 10$ kW/m^2), is the heat transfer coefficient affected by the vapor quality. The independency of the heat transfer coefficient on the vapor quality is different from the general trend observed in an in-tube convective boiling. For in-tube boiling, the heat transfer coefficient increases as the vapor quality increases up to $x = 0.8$ to 0.9, mainly due to the thinning of the annular film on the tube wall. The flow regime of the present study was checked using the flow regime map by Ulbrich and Mewes [12], which was developed from the air–water data in a tube bundle. The data were in a bubbly or in an intermittent flow regime. The photos taken during the tests also supported the finding. One notable thing from Ulbrich and Mewes' study is that an annular flow, which prevails over the quality for an in-tube flow, was not observed for the tube bundle flow. The independency of the heat transfer coefficient on the vapor quality is believed to be related with the flow pattern in the bundle. Inspection of Fig. 6 shows that the effect of mass velocity is not significant. The mass velocity effect is known to be significant only at a low heat flux combined with a high mass velocity [13]. The range of the present mass velocity (8–26 kg/m^2 s) was chosen considering the operation range of a refrigeration chiller [6].

Data taken at 26.7 °C saturation temperature are compared with those taken at 4.4 °C in Fig. 7. The mass flux is 26 kg/m^2 s. Data show approximately same

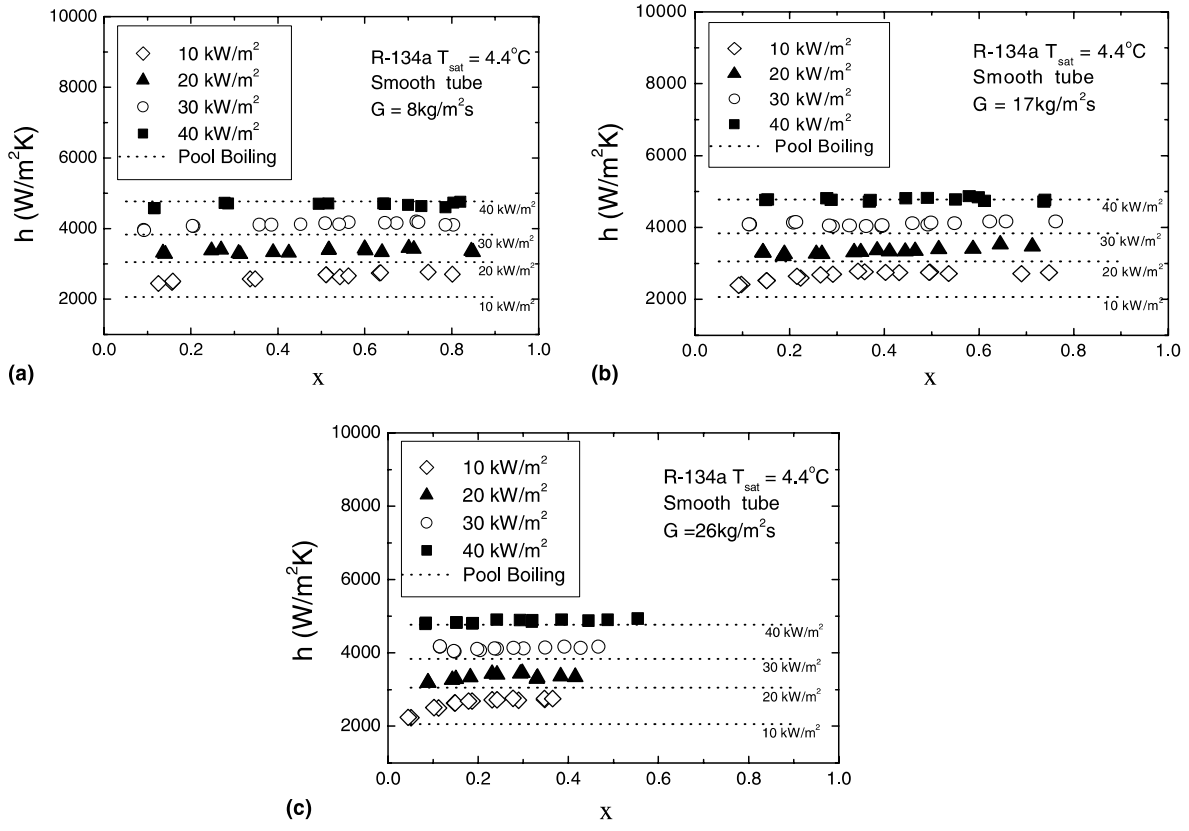

Fig. 6. Convective boiling heat transfer coefficients of the smooth tube bundle for R-134a at $T_{sat} = 4.4$ °C: (a) $G = 8$ kg/m^2 s; (b) $G = 17$ kg/m^2 s; (c) $G = 26$ kg/m^2 s.

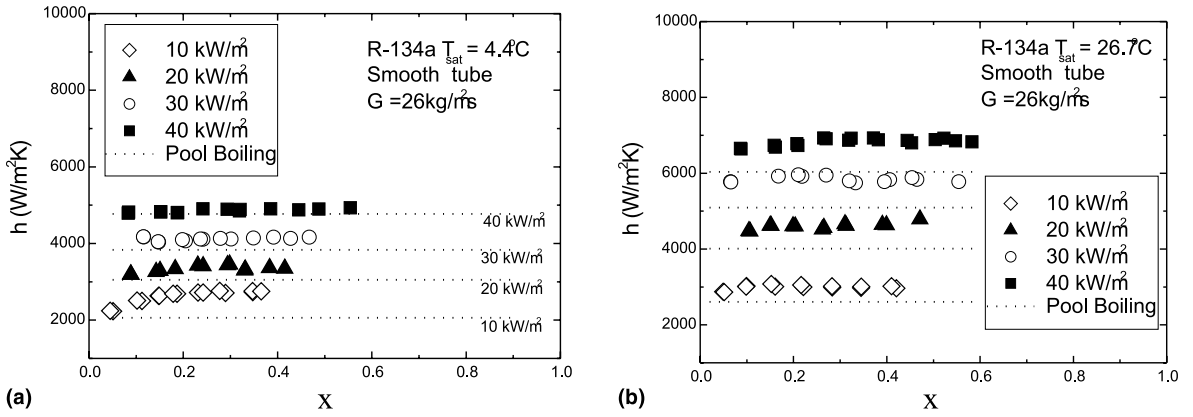

Fig. 7. Convective boiling heat transfer coefficients of the smooth tube bundle for R-134a at $G = 26$ kg/m^2 s: (a) $T_{sat} = 4.4$ °C; (b) $T_{sat} = 26.7$ °C.

trends on vapor quality and heat flux except that the heat transfer coefficient is higher at 26.7 °C. A higher pool boiling heat transfer coefficient at 26.7 °C [9] is believed to be responsible for the higher convective boiling heat transfer coefficient. The R-123 data are shown in Fig. 8. For R-123, data were taken at 26.7 °C because of the limitation on the condenser capacity. Similar trend – weak dependency on vapor quality and mass flux – is noticed except at a low mass flux, where the heat transfer coefficient slightly increases as the vapor quality increases.

The enhancement by convective effect in a bundle was defined by the bundle factor (h_b/h_{nbb}: convective boiling heat transfer coefficient divided by the pool

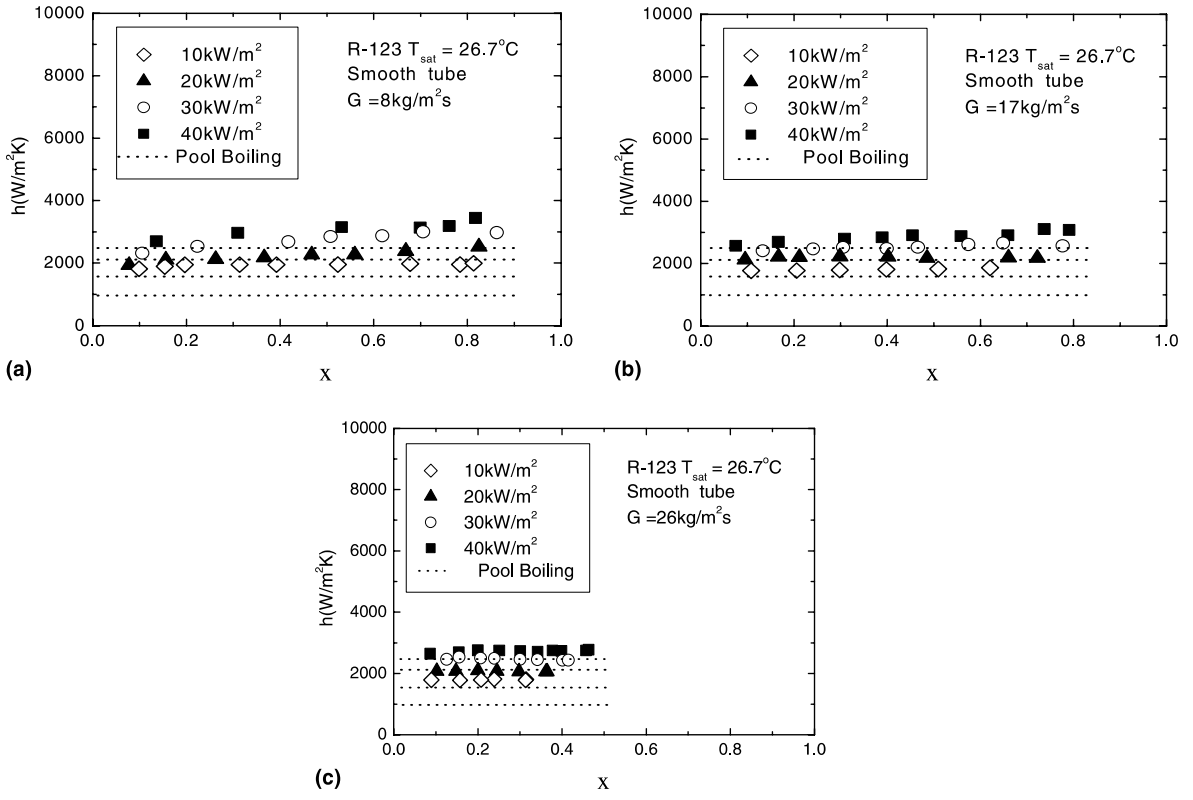

Fig. 8. Convective boiling heat transfer coefficients of the smooth tube bundle for R-123 at $T_{sat} = 26.7$ °C: (a) $G = 8$ kg/m^2 s; (b) $G = 17$ kg/m^2 s; (c) $G = 26$ kg/m^2 s.

boiling heat transfer coefficient), and is tabulated in Table 3. The h_b has been averaged on vapor quality, and h_{nbb} was obtained from the pool boiling test. Table 3 shows that, for the smooth tube bundle, most of the bundle factors are larger than 1.0, which indicates the importance of the convective contribution. The convective effect is seen to be more prominent at lower heat fluxes. The average bundle factors listed in the last column indicate that the effect of mass velocity is not significant. Comparing the bundle factors of R-134a and R-123, one may conclude that the convective effect is stronger for R-123. This trend is reversed for the enhanced tube bundle. Possible explanation will be provided in Section 5.3.

5.3. Convective boiling in enhanced tube bundles

The convective boiling data for the bundle of enhanced tubes were obtained for two different refrigerants (R-123, R-134a) at two different saturation temperatures (4.4 °C, 26.7 °C). Tubes having different pore size ($d_p = 0.20$, 0.23, 0.27 mm) were tested, and the results are shown in Figs. 9–13. Fig. 9 shows the data taken for the tube having the largest pores ($d_p = 0.27$ mm). The saturation temperature is 4.4 °C, and the refrigerant is R-134a. A similar trend to the smooth tube bundle – weak dependency on vapor quality and mass flux – is noticed. Only at low heat flux, does the heat transfer coefficient slightly increase as the vapor quality increases. Data taken at 26.7 °C are compared with those taken at 4.4 °C in Fig. 10. The mass flux is 26 kg/m^2 s. Both figures show a similar trend except that the heat transfer coefficients are higher at 26.7 °C. The R-123 data are shown in Fig. 11. For R-123, data were taken at 26.7 °C. Similar trend – weak dependency on vapor quality and mass flux – is noticed.

Figs. 12 and 13 show the effect of pore size. In Fig. 14, R-134a data at 4.4 °C and 26 kg/m^2 s are shown. Fig. 12 indicates that the highest heat transfer coefficient is obtained for the tube bundle having the largest pore diameter ($d_p = 0.27$ mm). The geometry also yielded the highest pool boiling heat transfer coefficient [9]. In Fig. 13, R-123 data are compared. The saturation temperature is 26.7 °C and the mass flux is 26 kg/m^2 s. Different from R-134a, the highest bundle heat transfer coefficient is obtained for the interim pore size ($d_p = 0.23$ mm). The pore size also yielded the highest pool boiling heat transfer coefficient for R-123 [9]. This point is more clearly illustrated in Fig. 14, where the heat transfer coefficients are plotted as a function of pore diameter. Both the bundle and the pool boiling heat transfer coefficients show a similar trend. For R-134a, the heat transfer coefficient increases as the pore diameter increases, which suggests that optimum pore diameter may be larger than 0.27 mm. More investigation is needed to clarify this.

The bundle factors are calculated from the data, and are listed in Table 3. Table 3 indicates that the bundle

Table 3
Summary of bundle factors of the present study

Tube	Refrigerant	T_{sat} (°C)	G (kg/m^{2}s)	Bundle factor (h_b/h_{nb}) kW/m^2				
				10	20	30	40	Avg.
		4.4	8	1.27	1.10	1.07	1.98	1.11
			17	1.29	1.09	1.07	1.00	1.11
	R-134a		26	1.27	1.09	1.07	1.02	1.11
Smooth		26.7	26	1.15	1.15	1.15	1.13	1.14
			8	2.00	1.42	1.30	1.24	1.49
	R-123	26.7	17	1.87	1.40	1.19	1.15	1.40
			26	1.86	1.32	1.18		1.45
$d_p = 0.27$ mm		4.4	8	1.09	1.13	1.10	1.04	1.09
			17		1.08	1.02	1.01	1.04
	R-134a		26	1.21	1.14	1.11	1.06	1.13
		26.7	26		1.19	1.14	1.17	1.17
			8	1.16	1.07	1.03		1.09
	R-123	26.7	17	1.19	1.09	1.02		1.10
			26	1.18	1.09	1.05	1.05	1.09
$d_p = 0.23$ mm		4.4	26	1.30	1.14	1.05	1.07	1.14
	R-134a	26.7	26	1.28	1.13	1.05	1.09	1.14
	R-123	26.7	26	1.02	1.03	1.01	1.03	1.02
$d_p = 0.20$ mm		4.4	26	1.26	1.15	1.13	1.16	1.17
	R-134a	26.7	26	1.33	1.25	1.33	1.26	1.29
	R-123	26.7	26	1.15	1.09	1.06	1.01	1.08

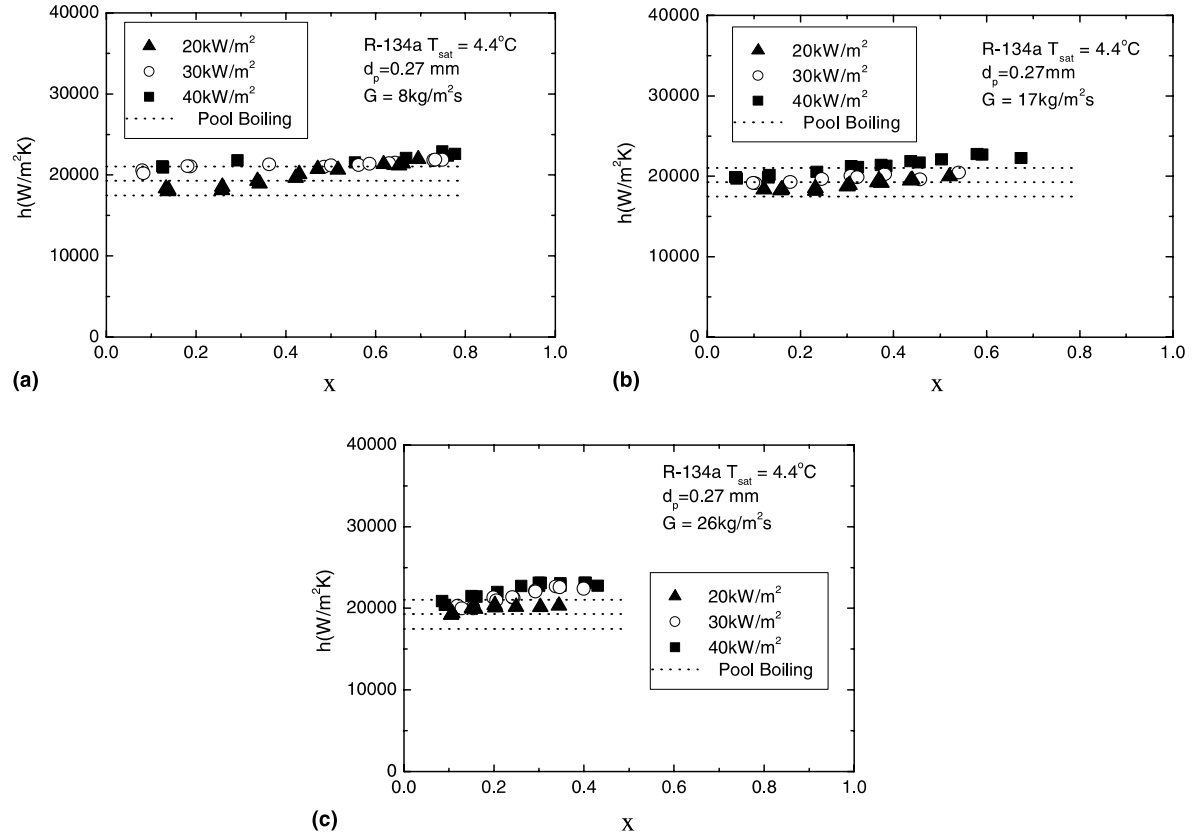

Fig. 9. Convective boiling heat transfer coefficients of the enhanced tube bundle ($d_p = 0.27$ mm) for R-134a at $T_{sat} = 4.4$ °C: (a) $G = 8$ kg/m^2 s; (b) $G = 17$ kg/m^2 s; (c) $G = 26$ kg/m^2 s.

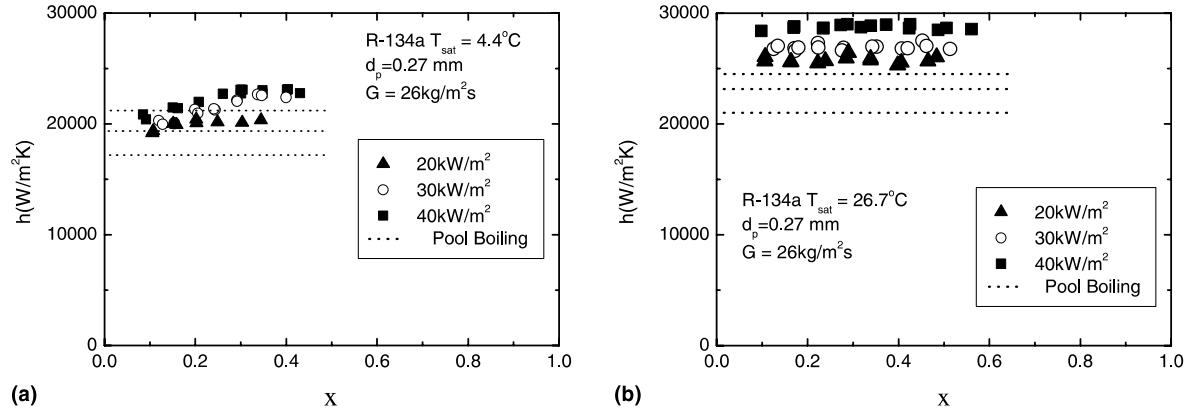

Fig. 10. Convective boiling heat transfer coefficients of the enhanced tube bundle ($d_p = 0.27$ mm) for R-134a at $G = 26$ kg/m^2 s: (a) $T_{sat} = 4.4$ °C; (b) $T_{sat} = 26.7$ °C.

factors of the enhanced tubes are larger than 1.0. As discussed previously, the present tubes have pores and connecting gaps. For the pore-only tube such as Turbo-B, Gupte and Webb [6] obtained the bundle factor not larger than 1.0. The gaps of the present tubes may have served routes for the passage of two-phase mixtures, and enhanced the boiling heat transfer.

Comparing the bundle factors at 26.7 and 4.4 °C, one may conclude that higher the saturation temperature goes, larger the bundle factor becomes. The reason may

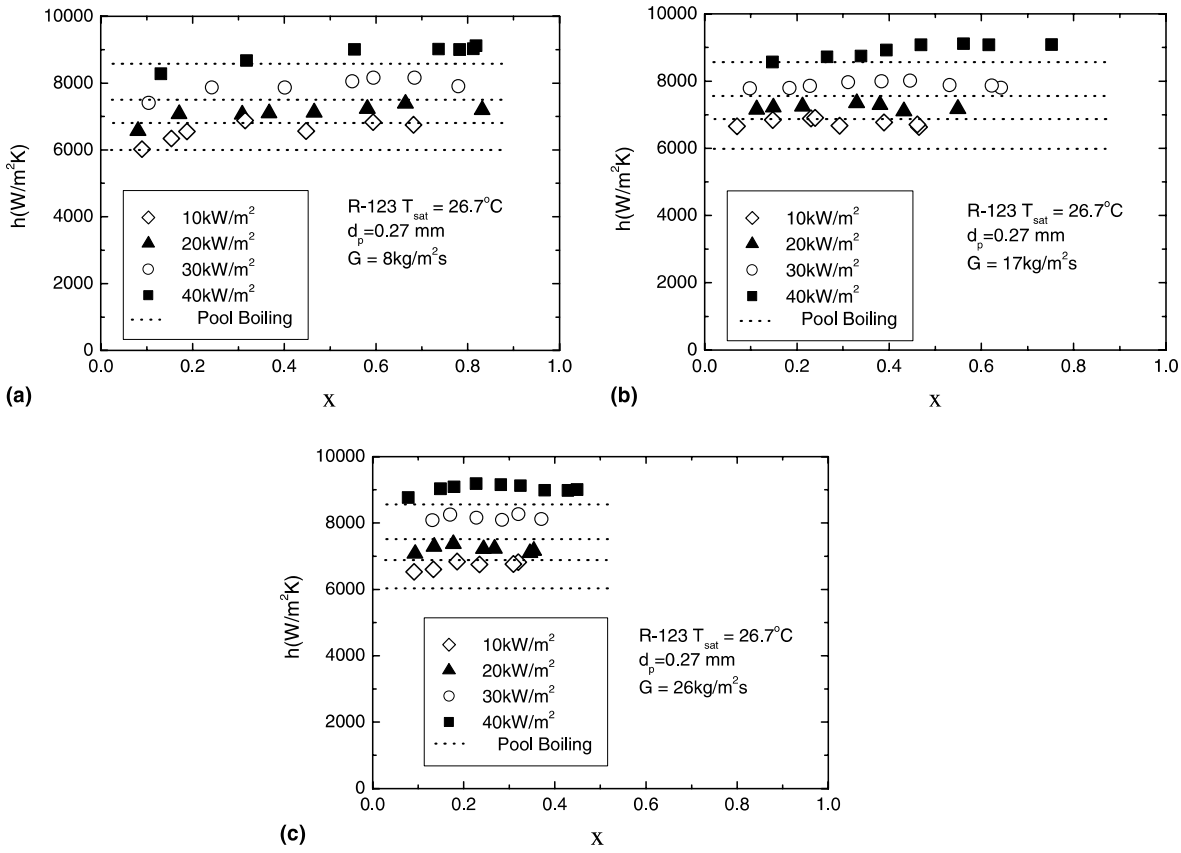

Fig. 11. Convective boiling heat transfer coefficients of the enhanced tube bundle ($d_p = 0.27$ mm) for R-123 at $T_{sat} = 26.7$ °C: (a) $G = 8$ kg/m^2 s; (b) $G = 17$ kg/m^2 s; (c) $G = 26$ kg/m^2 s.

be attributed to the improved pool boiling heat transfer performance at a higher saturation temperature [9]. More bubbles will be generated at a higher saturation temperature, which will lead to enhanced convective contribution. Table 3 shows that, for enhanced tube bundles, bundle factors for R-123 are smaller than those for R-134a. For the smooth tube bundle, the trend is reversed. The implication of bundle factor is the convective contribution, and will be strongly related with the bubble behavior on the wall. Generally, bubbles get smaller as the reduced pressure gets larger. The reduced pressure of R-123 is much smaller than that of R-134a, and the bubble size will be larger for R-123. Calculation using Cole's [14] model yielded that the bubble departure diameter ($d_b = 0.3$ mm) for R-123 is approximately six times larger than that ($d_b = 0.05$ mm) for R-134a at $T_{sat} = 26.7$ °C. The bubble generation frequency for R-134a is approximately five times larger than that for R-123. It is likely that a bubble diameter has more influence to the bundle factor than a bubble frequency. Larger bubbles will induce stronger convection currents, and thus yield larger bundle factor. This may explain why the bundle factor is larger for R-123 for the smooth tube bundle.

Different from the smooth tube, where bubbles are generated on the tube wall, bubbles are generated from the pores for enhanced tubes. The pore-generated bubbles are reported to have approximately the same size irrespective of refrigerants [15]. In addition, for a pored tube, the latent heat flux ratio (latent heat flux to the total heat flux) for R-134a is much greater than that for R-123 [16]. Greater latent heat will yield more bubbles. These will lead to larger bundle factors for R-134a for enhanced tube bundles. One more thing to note from Table 3 is that the pore diameter (or the corresponding gap width) does not have a discernable effect on the bundle factor. The range of gap width of the present tubes is from 0.04 to 0.1 mm.

In Fig. 15, the heat transfer coefficients of the present tubes are compared with those of other enhanced tubes [6]. The GEWA-SE is a gapped tube having 1062 fins/m, and Turbo-B is a pored tube having 1654 fins/m. The gap size of GEWA-SE or the pore size of Turbo-B is not provided in the paper [6]. The present enhanced tubes have 1654 fins/m. Fig. 15 indicates that the present tubes yield higher convective boiling heat transfer coefficients.

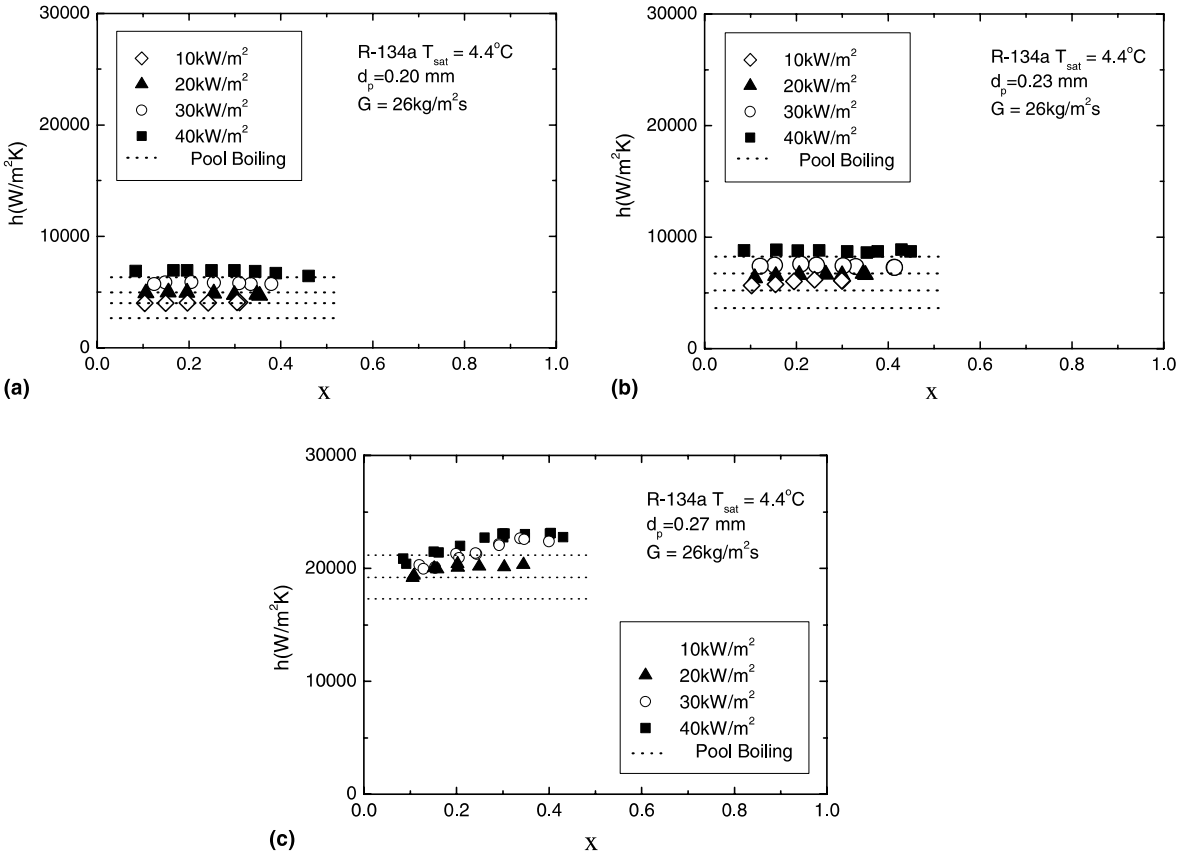

Fig. 12. Convective boiling heat transfer coefficients of the enhanced tube bundle for R-134a at $T_{sat} = 4.4$ °C, $G = 26$ kg/m^2 s showing the effect of pore size: (a) $d_p = 0.27$ mm; (b) $d_p = 0.23$ mm; (c) $d_p = 0.20$ mm.

5.4. Correlation of data

Contrary to the convective boiling in tubes, where a wide choice of correlations is available, the choice of correlations for tube bundles is very limited. Gupte and Webb [9] suggested that two models – the modified Chen model and the asymptotic model – are applicable to the convective boiling in a bundle. The modified Chen model adds the convective evaporation coefficient and the nucleate boiling coefficient to obtain the convective boiling coefficient:

$$h = Sh_{nb} + Fh_l. \tag{2}$$

Here, h_l is the liquid-phase heat transfer coefficient, h_{nb} is the nucleate boiling component, F is the two-phase convective multiplier and S accounts for the suppression due to forced convection. The h_l term was calculated using the Zukauskas et al. [17] correlation as follows:

$$Nu_l = 0.675 Re_l^{0.5} Pr_l^{0.36} (Pr_l/Pr_w)^{0.25}. \tag{3}$$

The constant 0.675 and the Reynolds number exponent 0.5 are recommended by Zukauskas et al. for the present Reynolds number range. The h_{nb} term was obtained from the curve-fits of the pool boiling data at the same wall super-heat. For the F factor, Gupte and Webb [6] suggest the Bennet and Chen [18] expression modified for tube bundles:

$$F = \left[\frac{\phi_l^2 (Pr_l + 1)}{2}\right]^{C_2}, \tag{4}$$

where C_2 is given by

$$C_2 = \frac{m}{2 - b} \tag{5}$$

in which, m is the Reynolds number exponent in the Nusselt number correlation (Zukauskas et al. correlation) and b is the Reynolds number exponent in the Blasius-type correlation for the friction factor. For the present test range, $m = 0.5$, $b = 0.474$, which yield $C_2 = 0.327$. The ϕ_l^2 is the two-phase friction multiplier given by Ishihara et al. [19] as follows:

$$\phi_l^2 = 1 + \frac{8}{X_{tt}} + \frac{1}{X_{tt}^2}. \tag{6}$$

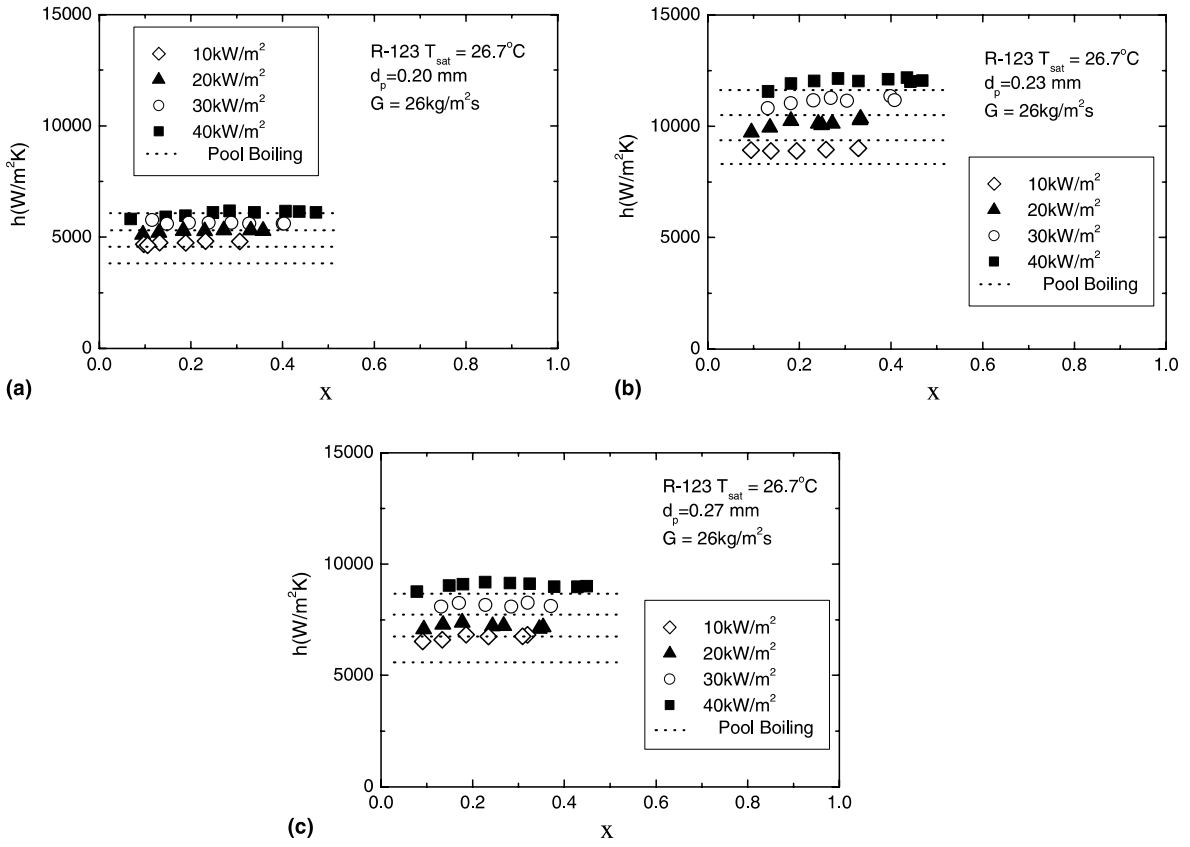

Fig. 13. Convective boiling heat transfer coefficients of the enhanced tube bundle for R-123 at $T_{sat} = 26.7\ ^{\circ}C$, $G = 26\ kg/m^2\ s$ showing the effect of pore size: (a) $d_p = 0.27$ mm; (b) $d_p = 0.23$ mm; (c) $d_p = 0.20$ mm.

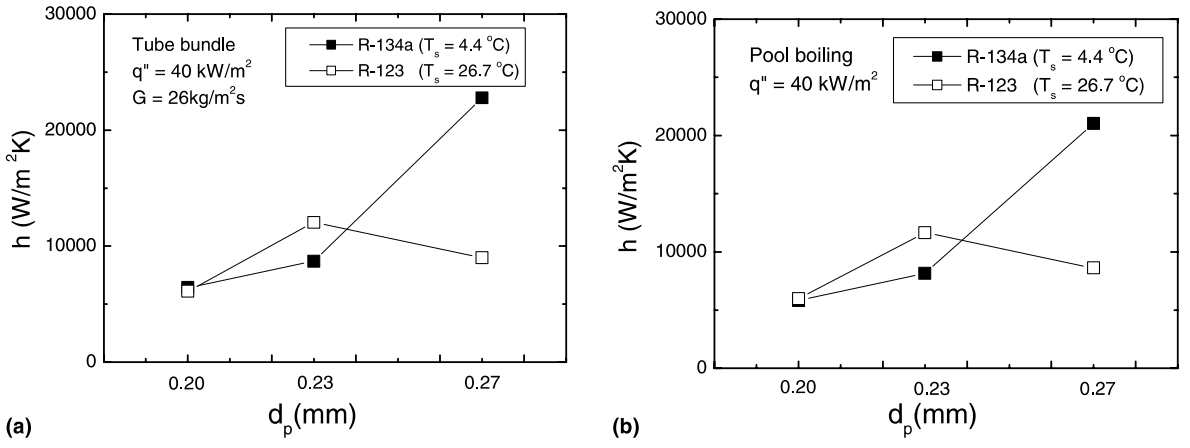

Fig. 14. Graphs showing the effect of pore diameter: (a) convective boiling; (b) pool boiling.

In Eq. (6), X_{tt} is the Martinelli parameter given by

$$X_{tt} = \left(\frac{1-x}{x}\right)^{0.9}\left(\frac{\rho_g}{\rho_l}\right)^{0.5}\left(\frac{\mu_l}{\mu_g}\right)^{0.1} \quad (7)$$

For the suppression factor S, Gupte and Webb [9] suggest $S = 1$ (no suppression) for enhanced tube bundles. They claimed that the nucleate boiling activity is governed by the sub-surface cavities for enhanced tubes, and thus these tubes are less likely to be

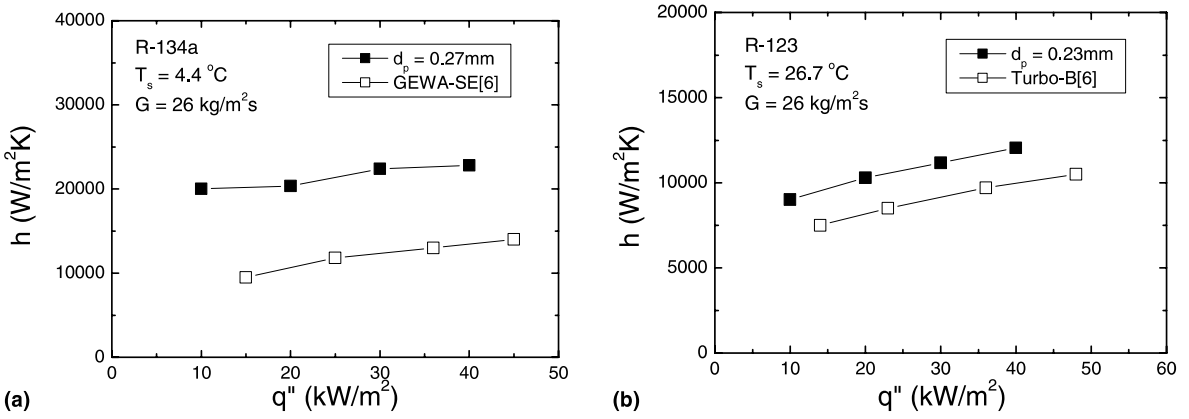

Fig. 15. Convective boiling heat transfer coefficients of the present enhanced tubes compared with those from other sources: (a) R-134a; (b) R-123.

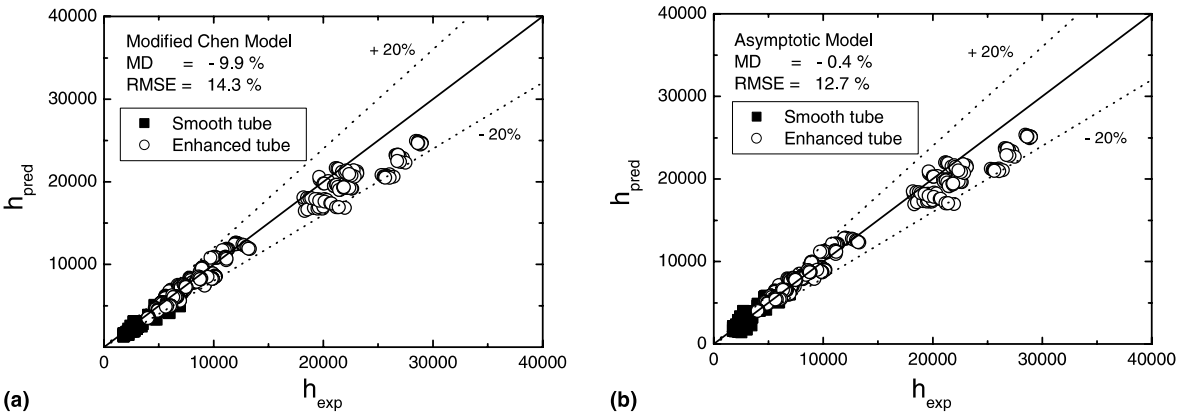

Fig. 16. The present data compared with existing models.

susceptible to external flow conditions. For a smooth tube bundle, however, the thermal boundary layer on the tube will get thinner as the vapor quality increases, and the boiling is likely to be suppressed. Webb and Chien [20] suggested the suppression factor by Bennet et al. [21] for the smooth tube bundle, which is as follows:

$$S = \left(\frac{k_l}{Fh_lX_0}\right)\left[1 - \exp\left(-\frac{Fh_lX_0}{k_l}\right)\right], \tag{8}$$

$$X_0 = 0.041\left[\frac{\sigma}{g(\rho_l - \rho_g)}\right]^{0.5}. \tag{9}$$

Fig. 16 shows that the modified Chen model predicts the present data reasonably well. The mean deviation (MD) is −9.9% with 44.5% of data predicted within ±10%, and 75.8% of data predicted within ±20%. The root mean square error (RMSE) is 14.3%. The MD and RMSE are defined as

$$\mathrm{MD} = \frac{\sum_1^N[(h_{\mathrm{pred}} - h_{\mathrm{exp}})/h_{\mathrm{exp}}]}{N}, \tag{10}$$

$$\mathrm{RMSE} = \sqrt{\frac{\sum_1^N[(h_{\mathrm{pred}} - h_{\mathrm{exp}})/h_{\mathrm{exp}}]^2}{N}}, \tag{11}$$

where h_{pred} and h_{exp} are the calculated and the experimental heat transfer coefficients, respectively.

The asymptotic model is given by the following expression:

$$h = \left[(Fh_l)^n + h_{\mathrm{nb}}^n\right]^{1/n}, \tag{12}$$

where n is called the order of the asymptotic model. The asymptotic model is generally used assuming $S = 1$, since the exponent n, which best fits the data, is chosen. The F factors are backed out from all the data using the following equation:

$$F = \frac{(h^n - h_{\mathrm{nb}}^n)^{1/n}}{h_l}. \tag{13}$$

These F factors are then correlated in the following form:

$$F = C_1 \left[\frac{\phi_l^2 (Pr_l + 1)}{2} \right]^{C_2}. \quad (14)$$

The F factor correlation is then used to calculate the MD and RMSE. This procedure has been repeated for several values of n. The best correlation was obtained for $n = 1$ yielding $C_1 = 2.70$ and $C_2 = 0.202$. Gupte and Webb [6] obtained $n = 3$ for the GEWA-SE and Turbo-B bundles. If $n = 1$, the asymptotic model has the same form as the modified Chen model. However, F factor correlations are different. For the modified Chen model, $C_1 = 1.0$ and $C_2 = 0.327$. For the asymptotic model, C_1 and C_2 are backed out from the experimental data. Therefore, better correlation is expected for the asymptotic model. In Fig. 16, the present data are compared with the predictions by the asymptotic model with $n = 1$. The MD is −0.4% and RMSE is 12.7%. The model predicts 55.6% of data within ±10%, and 91.0% of data within ±20%.

6. Conclusions

In this study, convective boiling tests were conducted for enhanced tube bundles. The surface geometry consists of pores and connecting gaps. Tubes with three different pore size ($d_p = 0.20$, 0.23 and 0.27 mm) were tested using R-123 and R-134a for the following range: 8 kg/m^2 s $\leqslant G \leqslant$ 26 kg/m^2 s, 10 kW/m^2 $\leqslant q \leqslant$ 40 kW/m^2 and $0.1 \leqslant x \leqslant 0.9$. Listed below are major findings:

1. The convective boiling heat transfer coefficients are strongly dependent on heat flux with negligible dependency on mass flux or quality.
2. The convective effect is apparent for the present enhanced geometry. The gaps of the present tubes may have served routes for the passage of two-phase mixtures, and enhanced the boiling heat transfer.
3. At a higher saturation temperature, the convective effect is more pronounced. More bubbles will be generated at a higher saturation temperature, which will lead to enhanced convective contribution.
4. The pore size where the maximum heat transfer coefficient is obtained is larger for R-134a ($d_p = 0.27$ mm) compared with that for R-123 ($d_p = 0.23$ mm). This trend is consistent with the previous pool boiling results.
5. For the enhanced tube bundles, the convective effect is more pronounced for R-134a than for R-123. The trend is reversed for the smooth tube bundle. Possible reasoning is provided based on the bubble behavior on the tube wall.
6. The present enhanced tubes yield higher convective boiling heat transfer coefficients compared with existing enhanced tubes.
7. Both the modified Chen and the asymptotic model predict the present data reasonably well. The RMSEs are 14.3% for the modified Chen model and 12.7% for the asymptotic model.

Acknowledgements

The fund for present study has been provided by the R&D Management Center for Energy and Resources of Korea. Technical assistance by Jong-Won Kim and Ho-Jong Jeong is appreciated.

References

[1] R. Roser, B. Thonon, P. Mercier, Experimental investigation on boiling of *n*-pentane across a horizontal tube bundle: two-phase flow and heat transfer characteristics, Int. J. Refrig. 22 (1999) 536–547.
[2] P.J. Marto, C.L. Anderson, Nucleate boiling characteristics of R-113 in a small tube bundle, J. Heat Transfer 114 (1992) 425–433.
[3] T.H. Hwang, S.C. Yao, Forced convective boiling in horizontal tube bundles, Int. J. Heat Mass Transfer 29 (5) (1986) 785–795.
[4] Z.-X. Li, E. Hahne, Boiling heat transfer on finned tube bundle with low tubes heated with constant heat flux, Exp. Thermal Fluid Sci. 11 (1995) 174–180.
[5] E. Hahne, J. Muller, Boiling on a finned tube and a finned tube bundle, Int. J. Heat Mass Transfer 26 (6) (1983) 849–859.
[6] N.S. Gupte, R.L. Webb, Convective vaporization data for pure refrigerants in tube banks, HVAC&R Research 1 (1) (1995) 48–60.
[7] S.B. Memory, N. Akcasayar, H. Eraydin, P.J. Marto, Nucleate pool boiling of R-114 and R-114-oil mixtures from smooth and enhance surfaces – II. Tube bundles, Int. J. Heat Mass Transfer 38 (8) (1995) 1363–1376.
[8] Y. Fujita, H. Ohta, S. Hidaka, K. Nishikawa, Nucleate boiling heat transfer on horizontal tubes in bundles, in: Proceedings of the 8th International Heat Transfer Conference, San Francisco, CA, vol. 5, 1986, pp. 2131–2136.
[9] N.-H. Kim, K.-K. Choi, Nucleate pool boiling on structured enhanced tubes having pores with connecting gaps, Int. J. Heat Mass Transfer 44 (1) (2001) 17–28.
[10] S.J. Kline, F.A. McClintock, The description of uncertainties in single sample experiments, Mech. Eng. 75 (1953) 3–9.
[11] R.L. Webb, C. Pais, Nucleate pool boiling data for five refrigerants on plain, integral-fin and enhanced tube geometries, Int. J. Heat Mass Transfer 35 (8) (1992) 893–1904.
[12] R. Ulbrich, D. Mewes, Vertical, upward gas–liquid two-phase flow across a tube bundle, Int. J. Multiphase Flow 20 (2) (1994) 249–272.
[13] M.K. Jensen, R.R. Trewin, A.E. Bergles, Cross flow boiling in enhanced tube bundles, in: S. Kakac, et al. (Eds.), Two-phase Flow in Energy Systems, ASME HTD, vol. 220, 1992, pp. 11–17.

[14] R. Cole, Bubble frequencies and departure volumes at subatmospheric pressures, AIChE J. 13 (1967) 779–783.
[15] L.-H. Chien, R.L. Webb, Measurement of bubble dynamics on an enhanced boiling surface, Exp. Thermal Fluid Sci. 16 (1998) 177–186.
[16] L.-H. Chien, R.L. Webb, Effect of geometry and fluid property parameters on performance of tunnel and pore enhanced boiling surfaces, J. Enhanced Heat Transfer 8 (2001) 329–340.
[17] A. Zukauskas, A. Skrinska, J. Zingzda, V. Gnielinski, Banks of plain and finned tubes, in: G.F. Hewitt (Ed.), Heat Exchanger Design Handbook, Begell House Inc., New York, 1998, Part II, Section 2.5.3.
[18] L. Bennet, J.C. Chen, Forced convective boiling in vertical tubes for saturated pure components and binary mixtures, AIChE J. 26 (3) (1980) 454–461.
[19] K. Ishihara, J.W. Palen, J. Taborek, Critical review of correlations for predicting two-phase flow pressure drop across tube banks, Heat Transfer Eng. 1 (3) (1980) 23–32.
[20] R.L. Webb, L.-H. Chien, Correlation of convective vaporization on banks of plain tubes using refrigerants, Heat Transfer Eng. 15 (3) (1994) 57–69.
[21] L. Bennet, M.W. Davies, B.L. Hertzler, The suppression of saturated nucleate boiling by forced convective flow, AIChE Symp. Ser. 76 (199) (1980) 91–100.